

Semiclassical approximation with zero velocity trajectories

Yair Goldfarb, Ilan Degani and David J. Tannor

Dept. of Chemical Physics, The Weizmann Institute of Science, Rehovot, 76100 Israel

Abstract

We present a new semiclassical method that yields an approximation to the quantum mechanical wavefunction at a fixed, predetermined position. In the approach, a hierarchy of ODEs are solved along a trajectory with zero velocity. The new approximation is local, both literally and from a quantum mechanical point of view, in the sense that neighboring trajectories do not communicate with each other. The approach is readily extended to imaginary time propagation and is particularly useful for the calculation of quantities where only *local* information is required. We present two applications: the calculation of tunneling probabilities and the calculation of low energy eigenvalues. In both applications we obtain excellent agreement with the exact quantum mechanics, with a single trajectory propagation.

I. INTRODUCTION

The first semiclassical method, the WKB method[1], was published almost simultaneously with the publication of the Schrödinger equation in 1926. Since then, semiclassical methods have continued to attract great interest for two primary reasons. First, semiclassical methods give insight into classical-quantum correspondence. Second, for large systems they hold the promise of significant computational advantages relative to full quantum mechanical calculations. In particular, in recent years much progress has been made in the chemical physics community in developing *time-dependent* semiclassical methods that are accurate and efficient for multidimensional systems. By semiclassical methods, one generally means the calculation of a quantum mechanical wavefunction or propagator via the propagation of classical (or classical-like) trajectories. Mathematically speaking, semiclassical methods cast the time-dependent Schrödinger equation (TDSE), which is a PDE, in terms of ODEs related to classical equations of motion. From a physical point of view, the semiclassical methods try to circumvent the non-locality of quantum mechanics.

In this paper we present a new method that is to some extent a cross between a numerical grid method and a semiclassical method. The method is derived by inserting a trial form $e^{iS/\hbar}$ into the TDSE and calculating the time-dependent complex phase at a *stationary* position. Since the method yields an approximate solution of the TDSE at a fixed position it is a cousin of grid methods. However, we compute S by solving a hierarchy of spatial derivatives of S along a stationary trajectory; information from the neighboring trajectories is incorporated only through the initial conditions. This property makes the approximation local from the quantum mechanical point of view, and hence a cousin of semiclassical methods. We refer to the new method as the zero-velocity complex action method (ZEVCA) since it employs a complex phase (action) and stationary trajectories.

The substitution of $e^{iS/\hbar}$ as an ansatz in the TDSE is the same starting point as several methods that are based on the hydrodynamic and Bohmian formulations of quantum mechanics[2, 3, 4, 5]. More specifically, ZEVCA is related to the Derivative Propagation Method[6], the Trajectory Stability Method[7] and Bohmian Mechanics with Complex Action[8]. As in the case with ZEVCA, these methods incorporate equations of motion for a hierarchy of spatial derivatives of the phase (and amplitude) that are calculated along trajectories. But unlike ZEVCA, in these other approaches the time dependent trajectories

propagate in either real or complex configuration space. The ZEVCA formulation employs fixed trajectories that yield the time dependence of the wavefunction at a *fixed, predetermined* position in configuration space. In reference [5] section 7.2, Wyatt considers the solution of the global hydrodynamic equations of quantum mechanics on fixed grid points (Eulerian grid) but he dismisses its usefulness as a numerical tool. The ZEVCA formulation shows how to obtain useful output of a local propagation at a single grid point.

For a number of quantum mechanical calculations, such as thermal rates or tunneling probabilities, knowledge of the wavefunction in all of configuration space is unnecessary: these quantities can be calculated by data at a single position or a small interval of space. For such calculations, ZEVCA has a significant numerical advantage since it produces local information at a predetermined position. The first application of ZEVCA that we present in this paper is the calculation of tunneling probabilities; ZEVCA is well suited for this calculation since tunneling probabilities can be calculated from a time integral of the probability current at a fixed position. The second application is the calculation of the lowest energy eigenvalue of a bound potential. For this application we make a minor modification to the ZEVCA formulation to adapt it to imaginary time propagation. In both applications we calculate the results by propagating *just a single trajectory*.

This paper is organized as follows. In section II we formulate ZEVCA for the real time Schrödinger propagator (section II A) and the imaginary time Schrödinger propagator (section II B). Since the multi-dimensional representation of ZEVCA is somewhat more complicated, we present only the one-dimensional derivation. Section III is dedicated to the implementation of ZEVCA for the derivation of tunneling probabilities (III A) and the first energy eigenvalue of a bound potential (III B). In section IV we present our summary and concluding remarks.

II. FORMULATION

A. The ZEVCA real time Schrödinger propagator

We start by inserting the ansatz[9, 10, 11]

$$\psi(x, t) = \exp \left[\frac{i}{\hbar} S(x, t) \right], \quad (2.1)$$

into the TDSE

$$i\hbar\psi_t = -\frac{\hbar^2}{2m}\psi_{xx} + V(x, t)\psi, \quad (2.2)$$

where $S(x, t)$ is a complex function, \hbar is Planck's constant divided by 2π , m is the mass of the particle and $V(x, t)$ is the potential energy function. The subscripts denote partial derivatives. The result is a quantum Hamilton-Jacobi equation[9, 10, 11]

$$S_t + \frac{1}{2m}S_x^2 + V = \frac{i\hbar}{2m}S_{xx}, \quad (2.3)$$

where we recognize the classical Hamilton-Jacobi equation on the LHS. On the RHS is an additional non-classical term that can be referred to as a "quantum potential". Our aim is to solve eq.(2.3) using the method of characteristics. This method is usually applied to the solution of first order PDEs. The underlying idea of the method of characteristics is to transform a single PDE (or a set of PDEs) to a set of ODEs that are solved along a characteristic curve. The characteristic is defined by setting a dependence between the independent variables of the PDE (or PDEs), in our case x and t . ZEVCA makes the simplest possible choice for the characteristics:

$$\frac{dx}{dt} = 0 \implies x(t) = x(0), \quad (2.4)$$

i.e. the characteristics are trajectories that remain at a constant position. The time dependence of the phase along the trajectory is given by inserting $S(x, t)$ in the Lagrangian time derivative defined as

$$\frac{d}{dt} \equiv \frac{\partial}{\partial t} + \frac{dx}{dt} \frac{\partial}{\partial x}. \quad (2.5)$$

The choice we made in eq.(2.4) equates the Lagrangian time derivative and the partial time derivative $\frac{d}{dt} = \frac{\partial}{\partial t}$. The result of the substitution is

$$\frac{dS}{dt} = S_t = \frac{i\hbar}{2m}S_{xx} - \frac{1}{2m}S_x^2 - V, \quad (2.6)$$

where we have used eq.(2.3). The integration of eq.(2.6) requires $S_x[x(0), t]$ and $S_{xx}[x(0), t]$. Note that the initial position $x(0)$ acts as a parameter. Defining

$$S_n[x(0), t] \equiv \left. \frac{\partial^n S}{\partial x^n} \right|_{[x(0), t]}, \quad (2.7)$$

we can write a general equation of motion for $S_n[x(0), t] \forall n$ in the following manner. We take the n^{th} spatial partial derivative of eq.(2.3)

$$(S_t)_n + \frac{1}{2m}(S_1^2)_n + V_n = \frac{i\hbar}{2m}S_{n+2}, \quad (2.8)$$

and insert the result in the time derivative of S_n

$$\frac{dS_n}{dt} = (S_t)_n = \frac{i\hbar}{2m} S_{n+2} - \frac{1}{2m} (S_1^2)_n - V_n, \quad (2.9)$$

where we have assumed that the time and spatial derivatives are interchangeable. Equation (2.9) reveals that the equation of motion of S_n depends on the result of two subsequent equations (by the dependence on S_{n+2}) and on all prior equations by the term $(S_1^2)_n = \sum_{j=0}^n \binom{n}{j} S_{j+1} S_{n-j+1}$. Hence, the general characteristic solution of eq.(2.3) yields an infinite hierarchy of ODEs defined by eqs.(2.9) where $n = 0, 1, \dots, \infty$. In other words, we have converted eq.(2.3) to an infinite set of local but coupled ODEs that generate the time dependence of the complex phase and its spatial derivatives at position $x(0)$. An approximation can now be obtained by truncating the set at some $n = N$; this is done by setting $S_{N+1} = S_{N+2} = 0$. We summarize the equations of motion of the ZEVCA approximation

$$\begin{aligned} \frac{dS_n}{dt} &= \frac{i\hbar}{2m} S_{n+2} - \frac{1}{2m} (S_1^2)_n - V_n[x(0)]; \quad n = 0, 1, \dots, N, \\ S_{N+1} &= S_{N+2} = 0, \end{aligned} \quad (2.10)$$

where we emphasize that the partial derivatives of the potential are taken at a fixed position $x(0)$. The initial conditions of eqs.(2.10) are given by

$$S_n[x(0), 0] = -i\hbar \left. \frac{\partial^n \ln[\psi(x, 0)]}{\partial x^n} \right|_{x(0)}. \quad (2.11)$$

where we used the relation $S(x, 0) = -i\hbar \ln[\psi(x, 0)]$ from ansatz (2.1). After we solve set (2.10), the wavefunction at $x(0)$ is given by

$$\psi[x(0), t] = \exp \left[\frac{i}{\hbar} S_0[x(0), t] \right]. \quad (2.12)$$

B. The ZEVCA imaginary time Schrödinger propagator

The imaginary time Schrödinger propagator takes the form $\exp \left[-\frac{\hat{H}\tau}{2} \right]$ where

$$\hat{H} = -\frac{\hbar^2}{2m} \frac{\partial^2}{\partial x^2} + V(\hat{x}). \quad (2.13)$$

Applying this operator to an initial function $\psi(x, 0)$ yields a "wavefunction" $\tilde{\psi}(x, \tau)$ that is a solution of a Schrödinger-like equation

$$-\frac{\hbar^2}{2m} \tilde{\psi}_{xx}(x, \tau) + V(x) \tilde{\psi}(x, \tau) = -2\tilde{\psi}_\tau(x, \tau), \quad (2.14)$$

where τ plays the role of time. The mapping of τ to pure imaginary time $\tilde{t} = -\frac{i\hbar}{2}\tau$ (hence the term—“imaginary time propagation”) transforms the last equation to the form of the TDSE

$$i\hbar\tilde{\psi}_{\tilde{t}}(x, \tilde{t}) = -\frac{\hbar^2}{2m}\tilde{\psi}_{xx}(x, \tilde{t}) + V(x)\tilde{\psi}(x, \tilde{t}), \quad (2.15)$$

where for simplicity we allow a slight misuse of notation $\tilde{\psi}(x, \tau) \rightarrow \tilde{\psi}(x, \tilde{t})$. At this stage we insert in eq.(2.15) an ansatz identical to eq.(2.1)

$$\tilde{\psi}(x, \tilde{t}) = \exp\left[\frac{i}{\hbar}\tilde{S}(x, \tilde{t})\right], \quad (2.16)$$

and apply the ZEVCA formulation (section II A). This yields equations identical to eqs.(2.10) and (2.11) with the only difference being $t \rightarrow \tilde{t}$.

III. MODEL APPLICATIONS

A. Tunneling probabilities

In this section we calculate tunneling probabilities form an Eckart barrier using a single trajectory propagation. The potential is given by

$$V(x) = \frac{D}{[\cosh(\beta x)]^2}, \quad (3.1)$$

where D is the barrier height and $1/\beta$ gives an estimate of the barrier width. The initial wavefunction is a Gaussian wavepacket

$$\psi(x, 0) = \exp\left[-\alpha_0(x - x_c)^2 + \frac{i}{\hbar}p_c(x - x_c) + \frac{i}{\hbar}\gamma_0\right], \quad (3.2)$$

where $1/\sqrt{\alpha_0}$ relates to the Gaussian width and $\gamma_0 = -\frac{i\hbar}{4}\ln(\frac{2\alpha_0}{\pi})$ takes care of the normalization. x_c and p_c are the average position and momentum respectively. The initial conditions of eqs.(2.10) are obtained by inserting eq.(3.2) in eqs.(2.11)

$$S_0(x, 0) = i\alpha_0\hbar(x - x_c)^2 + p_c(x - x_c) + \gamma_0, \quad (3.3)$$

$$S_1(x, 0) = 2i\alpha_0\hbar(x - x_c) + p_c,$$

$$S_2(x, 0) = 2i\alpha_0\hbar,$$

$$S_n(x, 0) = 0, \quad n \geq 3.$$

The final tunneling probability T for an initial wavefunction centered at $x_c \ll 0$ and having $p_c \geq 0$ is given by

$$T = \lim_{t \rightarrow \infty} T(t), \quad (3.4)$$

where

$$T(t) = \int_0^\infty |\psi(x', t)|^2 dx', \quad (3.5)$$

is the time-dependent tunneling probability. The integration initiates at $x = 0$ since this is the position of the maximum of the barrier. $T(t)$ can be expressed by a time integration of the probability current at $x = 0$. We show this by first writing the quantum mechanical continuity equation

$$\rho_t(x, t) = -J_x(x, t), \quad (3.6)$$

where $\rho \equiv |\psi|^2$ is the probability amplitude and the probability current J is given by

$$J = \frac{\hbar}{m} \Im(\psi^\dagger \psi_x). \quad (3.7)$$

By inserting $\rho(x, t)$ is eq.(3.5) we can write

$$\begin{aligned} T(t) &= \int_0^\infty \rho(x', t) dx' \\ &= \int_0^\infty dx' \int_0^t \rho_t(x', t') dt' \\ &= - \int_0^\infty dx' \int_0^t J_x(x', t') dt' \\ &= - \int_0^t dt' \int_0^\infty J_x(x', t') dx' = \int_0^t J(0, t') dt'. \end{aligned} \quad (3.8)$$

where in the third stage we used eq.(3.6) and in the forth stage we changed the order of the integration and performed the spatial integration. Inserting ansatz (2.1) in eq.(3.7) reveals that

$$J = \frac{|\psi|^2}{m} \Re(S_1) = \frac{1}{m} \exp \left[\frac{-2\Im(S_0)}{\hbar} \right] \Re(S_1), \quad (3.9)$$

where we have used the notation defined by eq.(2.7). Inserting eq.(3.9) in the final result of eq.(3.8) yields

$$T(t) = \frac{1}{m} \int_0^t \exp \left\{ \frac{-2\Im[S_0(0, t')]}{\hbar} \right\} \Re[S_1(0, t')] dt'. \quad (3.10)$$

Note that S_1 is readily obtained by the propagation of set (2.10). To calculate $T(t)$ we need to set N and solve eqs.(2.10) with initial conditions (2.11) at $x(0) = 0$. Inserting $S_0(0, t)$ and $S_1(0, t)$ in eq.(3.10) completes the derivation of the tunneling probability.

We turn to the numerical results. The parameters we insert in eqs.(3.1) and (3.2) are $D = 40$, $\beta = 4.3228$, $\alpha_0 = 30\pi$, $x_c = -1.5$, and $p_c = \sqrt{2mE}$ where $E = 20$ and $m = 30$. All quantities here and henceforth are given in atomic units, hence $\hbar = 1$. In fig.1 we illustrate the potential and the wavefunctions. Note that the initial wavefunction is located close to the barrier maximum, for reasons that we discuss below.

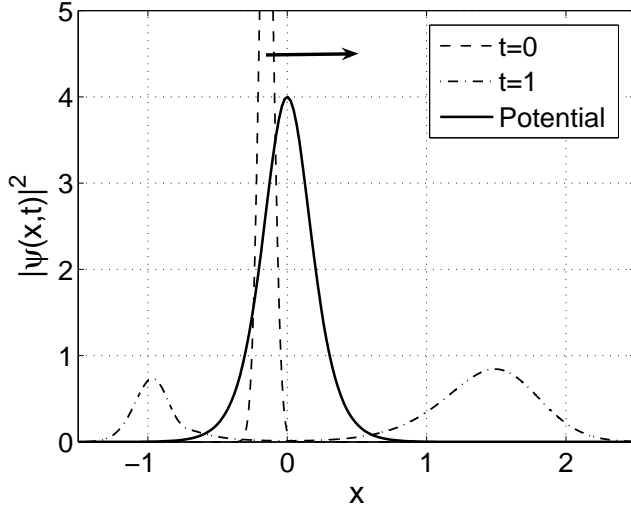


FIG. 1: Plot of an initial Gaussian wavefunction propagating in an Eckart barrier. At $t = 1$ where the wavefunction is clearly divided into a reflected part and a transmitted part. The depiction of the barrier's width is in proportion to that of the wavefunction, whereas the height of the barrier has no physical meaning. The arrow indicates the direction of the average average momentum. The parameters of the system are given in the text.

In figures 2(a) and 2(b) we depict the approximations to $|\psi(0, t)|^2$ and $T(t)$ for a series of values of the truncation order N . Note that $|\psi(0, t)|^2$ is equal to the exponential term in eq.(3.10). The relative error between the exact tunneling probability and the asymptotic value of $T(t)$ (see eq.(3.4)) for $N = 2$, $N = 6$, and $N = 10$ is roughly 20%, 4% and 0.5% respectively. Clearly, the numerical results converge quickly to the exact quantum mechanical result. In figures 3(a) and 3(b) we plot $|\psi(0, t)|^2$ and $T(t)$ for a set of N 's where we take $p_c = 0$. Although the relative error in the wavefunction $\psi(0, t)$ still converges uniformly, the relative error in $T(t)$ does not: the errors are 1.5%, 6% and 0.8% for $N = 2$, $N = 4$, and $N = 6$ respectively.

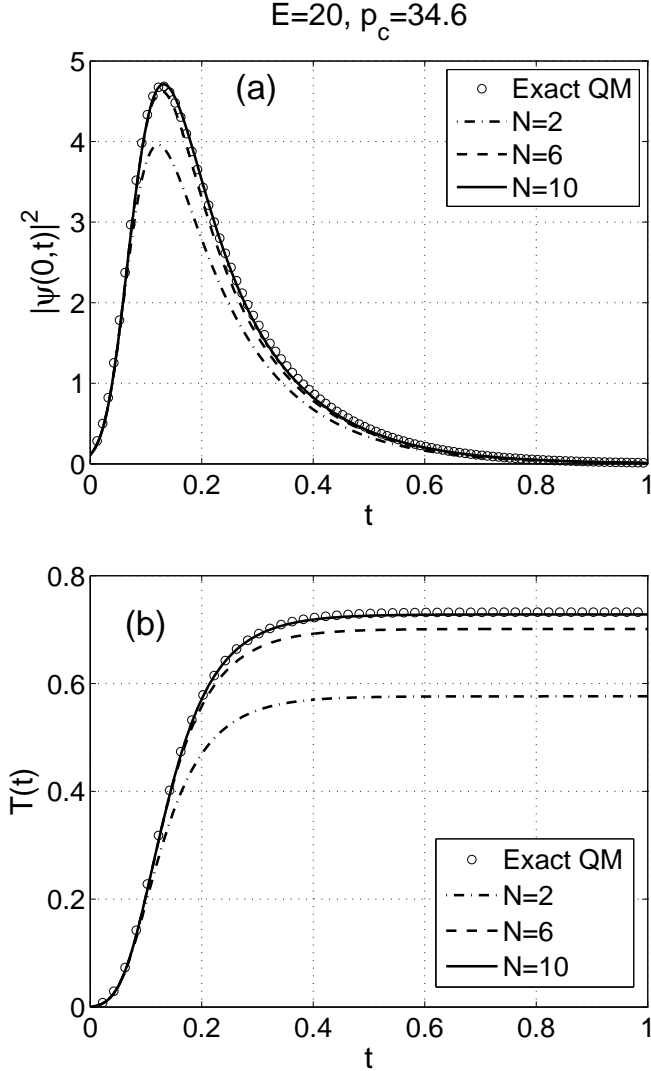


FIG. 2: ZEVCA numerical results for $|\psi(0,t)|^2$ ((a)) and the transmitted probability $T(t)$ ((b)) for a series of values of the truncation order N . The system corresponds to fig.1 where the exact parameters are given in the text. The relative error between the exact tunneling probability and the asymptotic value of $T(t)$ (see eq.(3.4)) for $N = 2$, $N = 6$, and $N = 10$ is roughly 20%, 4% and 0.5% respectively.

The ZEVCA formulation of tunneling probabilities has a significant restriction on its use. Since the ZEVCA trajectories remain fixed, the formulation is very sensitive to the initial conditions inserted in the equations of motion. The choice of $x(0)$ must satisfy two properties: (1) The derivatives of the potential ($V_n[x(0)]$, $n = 1, \dots, N$) must have at least one term that is significantly different from zero. (2) The initial wavefunction at $x(0)$

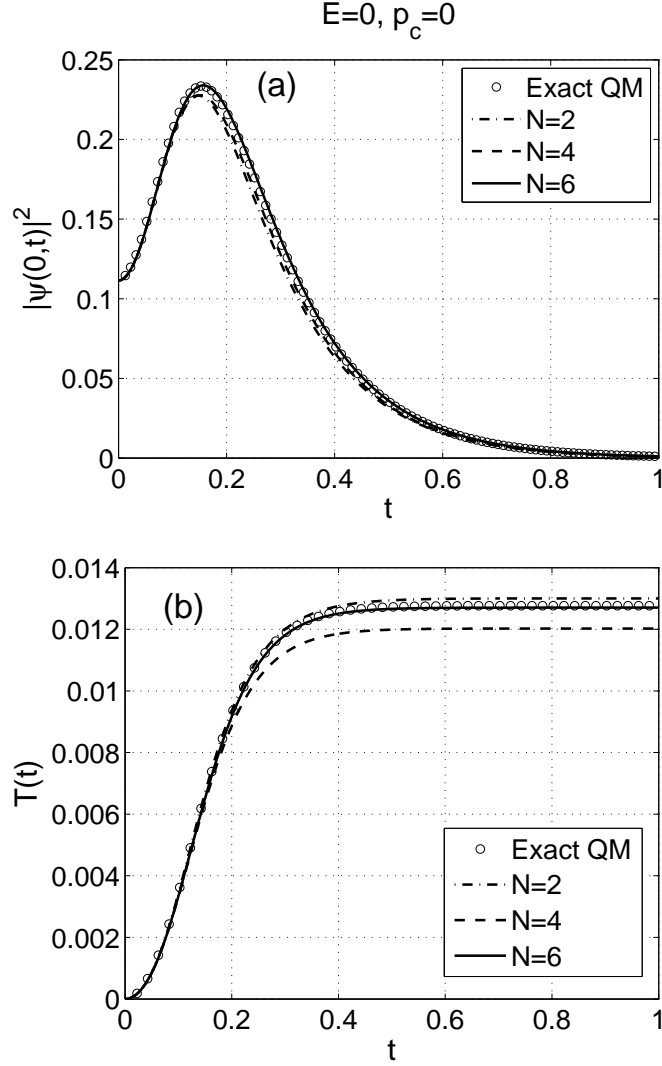


FIG. 3: Same as fig.2 expect that $p_c = 0$. The relative errors between the the exact tunneling probability and the asymptotic value of $T(t)$ (see eq.(3.4)) for $N = 2$, $N = 4$, and $N = 6$ are roughly 1.5%, 6% and 0.8% respectively.

$(\psi[x(0), 0])$ needs to be significantly different from zero. These restrictions ensure that the initial conditions "capture" the wavefunction and the potential's surroundings at $x(0)$. These restrictions have prevented us from choosing an x_c in the negative asymptotic region of the Eckart barrier since such a choice would have produced $\psi(0, 0) \rightarrow 0$.

B. Energy eigenvalues

The ZEVCA imaginary time propagator allows for a simple calculation of the first energy eigenvalue of a bound potential. As in the previous application, the calculation requires just a single trajectory propagation. We start with a short derivation that demonstrates how the first eigenvalue may be calculated using imaginary time propagation. An arbitrary bound potential defines a set of eigenfunctions $\phi_j(x)$, $j = 1, 2, \dots, \infty$ that satisfy $\hat{H}\phi_j(x) = E_j\phi_j$, where E_j are the energy eigenvalues and \hat{H} is given in eq.(2.13). The eigenfunctions can be used as a basis set for the expansion of an arbitrary wavefunction $\psi(x)$

$$\psi(x) = \sum_{j=1}^{\infty} a_j \phi_j(x), \quad (3.11)$$

where $\sum_{j=0}^{\infty} |a_j|^2 = 1$. If we define a time scale $\tau_1 = \frac{2\pi\hbar}{E_1}$ then the operation of the imaginary time propagator for $\tau \gg \tau_1$ on an initial wavepacket $\psi(x, 0)$ yields

$$\begin{aligned} \lim_{\tau \gg \tau_1} \exp \left[-\frac{\hat{H}\tau}{\hbar} \right] \psi(x, 0) &= \lim_{\tau \gg \tau_1} \exp \left[-\frac{\hat{H}\tau}{\hbar} \right] \sum_{j=1}^{\infty} a_j \phi_j(x) \\ &= \lim_{\tau \gg \tau_1} \sum_{j=1}^{\infty} a_j \phi_j(x) \exp \left[-\frac{E_j\tau}{\hbar} \right] \\ &= a_1 \phi_1(x) \exp \left[-\frac{E_1\tau}{\hbar} \right]. \end{aligned} \quad (3.12)$$

In the first stage we inserted eq.(3.11), in the second stage we applied the imaginary time propagator on the eigenfunctions and in the last stage we applied the limit. Inserting the relation $\tau = \frac{2i}{\hbar}\tilde{t}$ in the final result of eq.(3.12) and equating it with eq.(2.16) yields

$$a_1 \phi_1(x) \exp \left[-\frac{2iE_1\tilde{t}}{\hbar^2} \right] = \exp \left[\frac{i}{\hbar} \tilde{S}(x, \tilde{t}) \right], \quad (3.13)$$

hence,

$$\tilde{S}(x, \tilde{t}) = -\frac{2E_1\tilde{t}}{\hbar} - i\hbar \ln[a_1 \phi_1(x)]. \quad (3.14)$$

Taking the \tilde{t} partial derivative of the last equation yields

$$E_1 = -\frac{\hbar}{2} \tilde{S}_{\tilde{t}}(x, \tilde{t}), \quad (3.15)$$

where we recall that this relation holds for $\tau \gg \tau_1 \implies |\tilde{t}| \gg \hbar\tau_1$. As we mentioned in section II B, eqs.(2.10) hold for the imaginary time propagator with the substitution of $t \rightarrow \tilde{t}$. Hence,

$$E_1 = -\frac{\hbar}{2} \tilde{S}_{\tilde{t}} = -\frac{\hbar}{2} \frac{d\tilde{S}}{d\tilde{t}} = -\frac{\hbar}{2} \left[\frac{i\hbar}{2m} \tilde{S}_2 - \frac{1}{2m} (\tilde{S}_1)^2 - V \right]. \quad (3.16)$$

Since this equation holds for every choice of $x(0)$ we need to propagate only a single trajectory for a sufficiently long (imaginary) time \tilde{t} to calculate E_1 .

Liu and Makri have used a Bohmian related formulation, the trajectory stability method (TSM), to calculate energy eigenvalues [12]. TSM [7] emerges from conventional Bohmian mechanics by constructing a hierarchy of equations of motion for spatial derivatives of the phase and the amplitude of the wavefunction. In reference [12], Liu and Makri use TSM for imaginary time propagation at constant-position characteristics, as we do here. But the modification of TSM for imaginary time propagation is non-unique; moreover, producing constant-position characteristics is quite an elaborate procedure that must be repeated at every time step. In contrast, the ZEVCA transformation from the Schrödinger real time propagator to the imaginary time propagator is unique and the fixed characteristics are obtained for all time simply by *choosing* $\frac{dx}{dt} = 0$. As we demonstrate, the energy eigenvalues obtained using ZEVCA are of the same accuracy as using TSM while the formulation is decidedly simpler.

For the sake of comparison, we consider two of the potentials that were studied in reference [12]. The first is a quartic potential $V(x) = \frac{1}{2}x^2 + x^4$. The parameters of the Gaussian initial wavepacket (eq.(3.2)) are $\alpha_0 = 0.5$, $x_c = 1$ and $p_0 = 0$ with $m = 1$. The fixed trajectory that we propagate is at $x(0) = 0$. The results are very robust with respect to the choice of the initial parameters. In fig.4 we depict E_1 (eq.(3.16)) as function of τ ($\tau = \frac{2i}{\hbar}\tilde{t}$) for a series of values of the truncation order N . The relative error between the exact energy eigenvalue ($E_1 = 0.8038$) and the ZEVCA approximations are roughly 38%, 4% and 0.6% for $N = 2$, $N = 4$ and $N = 8$ respectively. For $N = 16$ the relative error reaches 0.1%. We see a clear convergence to the exact quantum mechanical result as a function of N .

The second example is a Morse potential $V(x) = D[1 - \exp(-\alpha x)]^2$. The parameters of the potential and the mass are $D = 0.1745$, $\alpha = 1.026$ and $m = 1837/2$. These parameters correspond to the vibration of an H_2 molecule. The parameters of the initial Gaussian wavepacket (eq.(3.2)) are $\alpha_0 = 4.5924$, $x_c = 0.1$ and $p_0 = 0$. The fixed trajectory is positioned at $x(0) = 0$. As in the previous example, the results are robust with respect to the choice of the initial Gaussian parameters and the position of the fixed trajectory, $x(0)$. In fig.5 we depict E_1 as function of τ for a series of values of the truncation order N . The relative error between the exact energy eigenvalue ($E_1 = 0.0098565$) and the ZEVCA approximations are roughly 1.4%, 0.08% and $2 \cdot 10^{-4}\%$ for $N = 2$, $N = 4$ and $N = 6$.

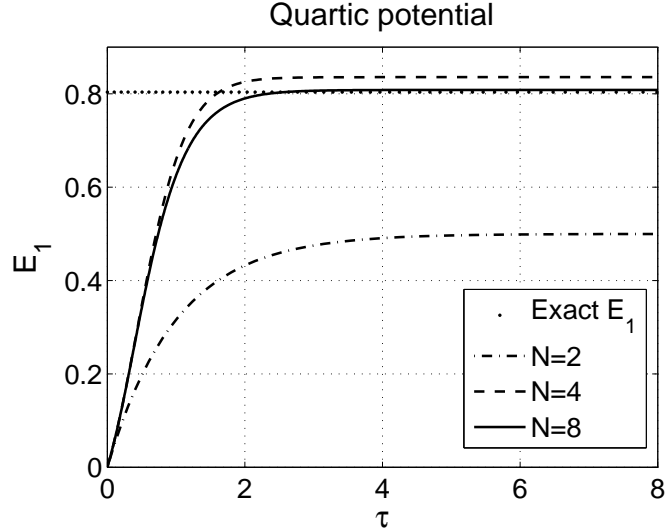


FIG. 4: A comparison between the exact lowest energy eigenvalue of a quartic potential and the results obtained using a the ZEVCA imaginary time propagator in eq.(3.16) with series of values of the truncation parameter N . The potential function is $V(x) = \frac{1}{2}x^2 + x^4$, where the numerical parameters appear in the text. The relative error between the exact energy eigenvalue ($E_1 = 0.8038$) and the ZEVCA approximations for $N = 2$, $N = 4$ and $N = 8$ is roughly 38%, 4% and 0.6% respectively.

respectively. In this example we see a faster convergence to the exact result as a function of N than in the quartic case. The reason is that the parameters of the Morse potential correspond to a small perturbation from a harmonic oscillator potential. For the harmonic oscillator it is possible to show that the ZEVCA approximation for $N = 2$ yields the exact quantum result. For anharmonic oscillators, the truncation at $N = 2$ incorporates only $V_j[x(0), 0]$, $j = 0, 1, 2$ in eqs.(2.10), which is equivalent to making a harmonic approximation to the potential (note that the results obtained for $N = 2$ for both the quartic potential and the Morse potential correspond to the energy eigenvalue of the harmonic approximation to the two potentials respectively). Since the parameters of the Morse potential correspond to a smaller perturbation from a harmonic oscillator potential than the parameters for the quartic potential, the convergence with N is faster.

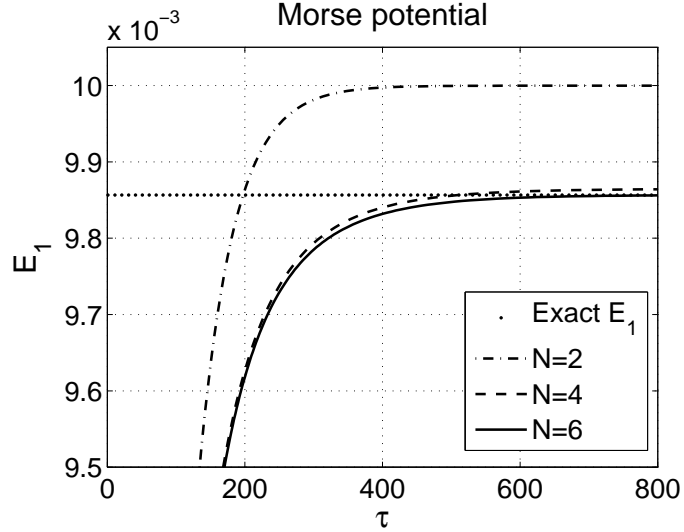


FIG. 5: A comparison between the exact lowest energy eigenvalue of a Morse potential and the results obtained by using the ZEVCA imaginary time propagator in eq.(3.16) with series of values of the truncation parameter N . The Morse potential parameters correspond to the vibration of an H_2 molecule (the numerical parameters appear in the text). The plot is a zoom of a complete graph that initiates at $\tau = 0$, $E_1 \simeq 4.5 \cdot 10^{-3}$. The relative error between the exact energy eigenvalue ($E_1 = 0.0098565$) and the ZEVCA approximations is roughly 1.4%, 0.08% and $2 \cdot 10^{-4}\%$ for $N = 2$, $N = 4$ and $N = 6$ respectively.

IV. SUMMARY

We have presented ZEVCA, a new approximation for quantum dynamics calculations that is a cross between a grid method and a semiclassical method. The formulation was applied to the calculation of tunneling probabilities and low energy eigenvalues, with surprisingly good accuracy. The ZEVCA formulation has several advantages: (1) The derivation of the formulation is straightforward and the equations of motion are readily solvable by standard numerical software. (2) The ZEVCA approximation yields the solution of the TDSE at a fixed and predetermined position. This allows for easy application to quantum quantities that require only local information. (3) The ZEVCA formulation requires the calculation of the potential and its derivatives only at $x(0)$ (see eqs.(2.10)). This is in contrast to most semiclassical methods that propagate trajectories in configuration space and require the calculation of the potential (or its derivatives) at each time step. (4) No root search

is needed as in many other semiclassical methods. (5) The extension to imaginary time propagation is easily attainable. (6) By taking $N \rightarrow \infty$, ZEVCA formally gives the exact quantum result. Although we have not conducted a rigorous comparison of timings, for the applications presented here ZEVCA was found to be several orders of magnitude faster than the exact quantum calculation using a Split Operator method.

Still, the numerical implementations reveals a number of limitations. First, the convergence to the exact result as a function of N seems to be asymptotic, in the sense that there is an optimal choice of N . Second, the method has difficulty at nodal positions. Surprisingly, this is not a result of the original ansatz (eq.(2.1)) but is a limitation imposed by the condition of fixed trajectories. Since the trajectories are fixed, clearly they cannot cross. We have demonstrated elsewhere that making the ansatz (2.1) but allowing for contributions from crossing trajectories can produce interference effects such as nodes and oscillations[13]. Third, in section III A we have presented limitations on the relation between the position of the initial wavefunction, the derivatives of the potential and the choice of $x(0)$. These limitations originate from the need to incorporate in the initial conditions of ZEVCA "sufficient" data for a successful propagation.

An alternative to the procedure we have described is to discard ansatz (2.1) and construct a hierarchy of ODEs for the wavefunction $\psi_n[x(0), t]$ itself, instead of for the complex phase, $S_n[x(0), t]$. We have explored this direction but found that it produces very poor results. In the case of an initial Gaussian wavepacket it is readily verified that the truncation for $N \geq 2$ does not entail any approximation to the complex phase derivatives $S_n[x(0), 0]$ (see eqs.(3.3)). This is not the case for the derivatives of the initial wavefunction $\psi_n[x(0), 0]$ itself, which go to infinity as a function of N for every choice of $x(0)$. This observation provides additional justification for making the replacement $\psi \rightarrow e^{iS/\hbar}$ in the first place.

We are currently working on several extensions of the ZEVCA formulation. Specifically, we are exploiting the local properties of ZEVCA for the calculation of thermal rates[14]. Similar to the implementations of ZEVCA we have presented in this paper, the calculation of thermal rates requires only local information. This allows us to obtain thermal rates for one-dimensional systems using only two trajectory propagations. We aim at exploring both ZEVCA and its close relative, Bohmian Mechanics with Complex Action, in multi-dimensional quantum systems.

This work was supported by the Israel Science Foundation (576/04).

- [1] G. Wentzel, Z. Phys. **38**, 518 (1926); H. A. Kramers, Z. Phys. **39**, 828 (1926); L. Brillouin, CR Acad. Sci, Paris **183**, 24 (1926); L. Brillouin, J. Phys., **7**, 353 (1926).
- [2] D. Bohm, Phys. Rev. **85**, 166 (1952); D. Bohm, Phys. Rev. **85**, 180 (1952)
- [3] D. Bohm, B. J. Hiley, *The Undivided Universe: An Ontological Interpretation of Quantum Theory* (Routledge, London, 1993)
- [4] P. R. Holland, *The Quantum Theory of Motion* (Cambridge University Press, Cambridge, 1993)
- [5] R. E. Wyatt, *Quantum Dynamics with Trajectories: Introduction to Quantum Hydrodynamic* (Springer, New York, 2005).
- [6] C. J. Trahan, K. Hughes, R. E. Wyatt, J. Chem. Phys. **118**, 9911 (2003).
- [7] J. Liu, N. Makri, J. Phys. Chem. A. **108**, 5408 (2004).
- [8] Y. Goldfarb, I. Degani, D. J. Tannor, J. Chem. Phys. **125**, 231103 (2006).
- [9] W. Pauli, *Die allgemeine Prinzipien der Wellenmechanik*, Encyclopedia of Physics, Vol. 5, Springer, Berlin, 1958.
- [10] K. Gottfried *Quantum Mechanics, Volume I: Foundations* (W. A. Benjamin, New York, 1966)
- [11] D. J. Tannor, *Introduction to Quantum Mechanics: A Time Dependent Perspective* (University Science Press, Sausalito, 2007).
- [12] J. Liu, N. Makri, Molecular Physics, **103**, 1083 (2005).
- [13] Y. Goldfarb, J. Schiff, D. J. Tannor, (In preparation).
- [14] Y. Goldfarb, I. Degani, D. J. Tannor, (In preparation).